ΕΝΤΟΠΙΣΜΟΣ ΓΕΩΛΟΓΙΚΩΝ ΣΧΗΜΑΤΙΣΜΩΝ ΜΕ ΕΠΕΞΕΡΓΑΣΙΑ ΥΠΕΡΦΑΣΜΑΤΙΚΗΣ ΕΙΚΟΝΑΣ ΣΤΗ ΝΗΣΟ ΝΑΞΟ.

Χάρου Ε.[1], Στεφούλη Μ.[2], Χελιώτης Ι.[2]

[1] Ινστιτούτο Πληροφορικής και Τηλεπικοινωνιών – ΕΚΕΦΕ "Δημόκριτος"
[2]Ινστιτούτο Γεωλογικών και Μεταλλευτικών Ερευνών

Περίληψη

Κατά τη διάρκεια εκτέλεσης του προγράμματος λήψης δεδομένων με χρήση του HYMAP υπερφασματικού σαρωτή από το Γερμανικό Κέντρο Αεροδιαστημικής (DLR), πραγματοποιήθηκε η κάλυψη με δύο πτήσεις, επιλεγμένης ζώνης με διεύθυνση Ανατολή-Δύση στο κεντρικό τμήμα της Νήσου Νάξου. Στην εργασία που ακολουθεί γίνεται επεξεργασία της εικόνας του αερομεταφερόμενου υπερφασματικού δέκτη HYMAP για την εντοπισμό ορυκτών και την χαρτογράφηση πετρωμάτων στη νήσο Νάξο. Για την μείωση του αριθμού των καναλιών εφαρμόζεται ο Minimum Noise Fraction μετασχηματισμός. Δημιουργείται φασματική βιβλιοθήκη από αναγνωρίσιμα πετρώματα η οποία χρησιμοποιείται για την εφαρμογή των αλγορίθμων ταξινόμησης Spectral Angle Mapper και Matched Filtering. Τέλος χαρακτηριστικά φάσματα από την USGS φασματική βιβλιοθήκη εξετάζονται για τον εντοπισμό ορυκτών. Τα αποτελέσματα αξιολογούνται με την βοήθεια Γεωλογικού χάρτη και πρόσθετων πληροφοριών. Πιστοποιείται η δυνατότητα χαρτογράφησης διαφορετικών τύπων πετρωμάτων και προσδιορισμού ορυκτών στις ακολουθίες μαρμαροφόρων-δολομιτικών και παρεμβαλλόμενων μαρμαρυγιακών σχιστολιθικών, αμφιβολιτικών πετρωμάτων.

GEOLOGICAL FORMATION IDENTIFICATION USING HYPERSPECTRAL IMAGERY OF NAXOS ISLAND, GREECE

Charou E.[1], Stefouli M.[2], Cheliotis I.[2]

[1] Inst. of Informatics and Telecommunications, N.C.S.R. "Demokritos"
[2] Institute of Geology and Mineral Exploration.

Abstract

In 2005, flight campaign conducted by the German Aerospace Center (DLR) recorded 2 transects across the island of Naxos using the airborne hyperspectral scanner HYMAP. A pilot area has been selected in order to assess the geologic mapping and mineral identification capabilities of the HYMAP data. The pilot area covers all the major litho-tectonic units of interest, which is a metamorphic dome with the transition of metamorphic zonations from the outer meta-sedimentary greenschist envelope to the gneissic amphibolite facies and migmatitic core. Data have been converted from radiance to reflectance and noise filtered based on Minimum Noise Fraction. A spectral library with spectra of recognizable rock types was created. The Spectral Angle Mapper and Matched Filtering algorithms were tested for mineral identification. Finally characteristic spectra from USGS spectral library were used to identify minerals in the image. Results are discussed in comparison with existing geological map and additional information. Mapping lithologic units and mineral identification of alternating marble-dolomite sequences and interlayered schists bearing muscovite and biotite has been accomplished using the airborne hyperspectral HYMAP sensor.

Λέξεις κλειδιά: Τηλεπισκόπιση, Υπερφασματικά, HYMAP, Νάξος.

Key words: Remote sensing, Hyperspectral, HYMAP, Naxos.

1.Introduction

Hyperspectral analysis has been applied to mapping vegetation types (Lewis et al 2001), in water studies (Καραθανάση, κ.ά., 2005) and has proven particular valuable in geological mapping (Van, der Meer 2007, Ganas et all, 2002; Echtler et all, 2002; Taylor et all 2001). This study investigates the use of HYMAP data for the identification of geological formations in Naxos island, Greece. Naxos is the largest island of the Cycladic group of Eastern Greece. These islands form a curved belt of metamorphic rocks, known as the Attic-Cycladic Massif (ACM) which may be traced northwards on to the Greek mainland (Attika). Its extent eastwards is regarded to be the Menderes Massif of Turkey. Naxos is dominated by an elliptically-shaped structural and thermal dome, which was formed during late Tertiary deformation and metamorphism, and which was subsequently intruded on its western edge by a granodiorite. The metamorphic complex is considered to comprise two sequences in tectonic contact (Bonneau et al. 1978). The lower sequence forms the high-grade migmatitic core of the complex, whilst the upper sequence forms the lower grade envelope to the core. The granodiorite body which outcrops on the west side of the island was intruded into the cooling pile of rocks at about 13 Ma ago (Wijbrans 1985), inducing a narrow (max. 1 km) thermal metamorphic aureole. Shortly after the intrusion of the granodiorite, nonmetamorphic clastic sediments were tectonically emplaced upon the granodiorite and the metamorphic complex. There is evidence for a pronounced north-northeast (~15^0) stretching developed in the metapelitic rocks of Naxos. Almost all linear mesoscopic and megascopic fabric elements of the rocks trend in this direction e.g. fold axes and intersection lineations, mineral stretching lineations, the elongation direction defined by boudinage and the long axis of the migmatite dome itself. The dome rock suit consists of interbedded mica-schists and gneisses, marbles (ranging in composition from pure calcite to pure dolomite rocks), amphibolites and migmatites as well as basic and ultrabasic small bodies. They are classified into low grade (mica-schists and marbles) and high grade (amphibolites, marbles, and migmatites). Emery (metamorphic bauxite) deposits are found within marble horizons. Micas, quartz, plagioclase, chlorite, epidote are the main minerals in mica-schists, amphiboles and pyroxenes (hornblende, auger) and plagioclase are the main minerals in amphibolites. Tremolite, chlorite, actinolite are found at the periphery of serpentine and basic bodies. Granites consist of two micas, acid plagioclase and quartz. The selected part of the acquired Hymap image (Fig. 1) has been used in order to cover various major litho-tectonic units. Starting from the granodiorite which occupies the NW part of the image area and going to SE, there is part of the dome with metamorphic rock sequences from the outer meta-sedimentary greenschist envelope to the gneissic amphibolite facies and migmatitic core as shown in Figure 2. In the current work identification of the various lithologies along with the mineral identification of alternating marble-dolomite, two mica and amphibolitic schists using hyperspectral imagery is attempted. Results are discussed in comparison with detailed geological mapping and additional information.

Fig. 1. The HYMAP transect across the island of Naxos. 1: the pilot project area

2.Data description

In August 2005, flight campaign conducted by the German Aerospace Centre (DLR) recorded 2 transects across the island of Naxos using the airborne hyperspectral scanner HYMAP. The airborne scanner was configured to acquire data in 128 bands covering the range 445nm to 2447nm with the spectral resolution averaging 12-18nm. The data was flown at an elevation that gave approximately 6 m spatial resolution. The image was acquired in a clear summer day in order to minimise contribution of the clouds and vegetation. From the original data cube, 10 HYMAP spectral channels with high noise were identified as bad bands and removed from the data set. Consequently, subsequent analyses were restricted to the remaining 118 bands. The data was provided without any geo-referencing. A small part of the HYMAP scene was selected as pilot study area. All processing was carried using the TNTLITE free software package.

A freely available Landsat image was used for data fusion and comparison with Hymap imagery. The corresponding geologic map of the edition was converted from analogue to digital and used in order to acquire information and compare with the results obtained from the processing of data.

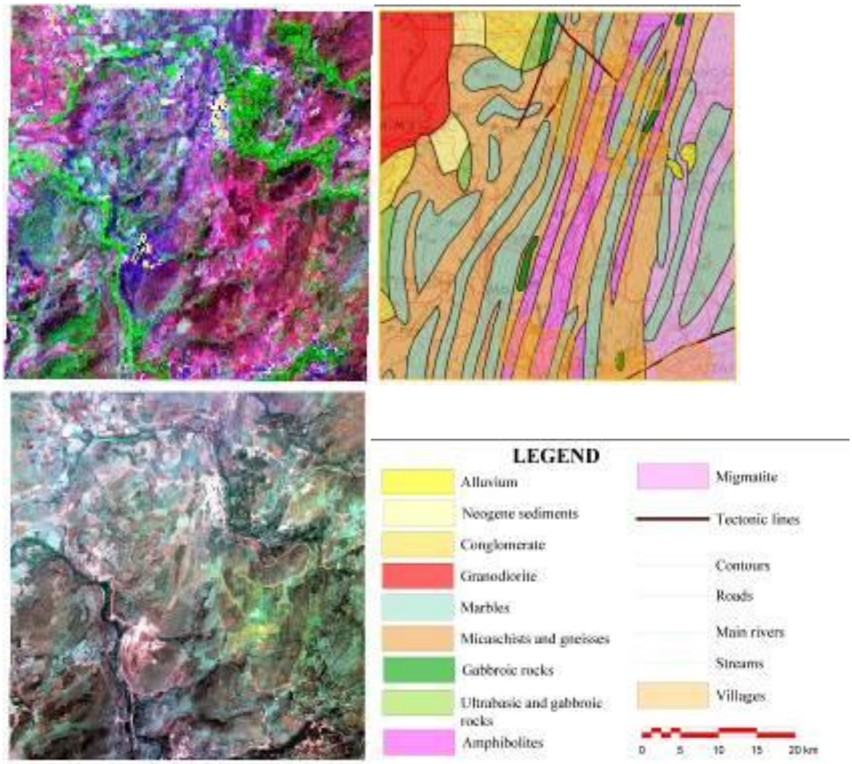

Fig. 2. The Landsat image (upper left), the HYMAP (down left) and the corresponding Geological map of the pilot project area (Jansen, 1973). Visual interpretation of both the Landsat ETM and HYMAP images makes possible the identification of the various lithological horizons, while the improved spatial resolution of the HYMAP data give better results.

3.Methodology

Methodology includes 3 main paths of actions; A) Data Reduction B) Creation of a library with spectra of recognizable rock types for the classification of the image and C) Acquisition of characteristic minerals spectra using the USGS spectral library.

3.1 Pre-processing

Atmospheric correction and additive offset calibration methods were applied to at sensor radiance values in order to convert them in reflectance and make comparisons between image spectra and laboratory reflectance spectra. There are generally 3 approaches available for atmospheric correction of hyperspectral imagery 1) image based methods such as log residuals, equal area normalization etc. 2) empirical methods, such as Empirical Line Method, which require ground measurements and 3) model-based correction methods which require special software such as ACORN, FLAASH etc. In our study the Equal Area Normalization method was used. According to this calibration method, the radiance values in each image spectrum are first scaled so that the sum of the values for each image cell is constant over the entire scene. This procedure shifts all image spectra to nearly the same relative brightness, removing differences in overall brightness between materials as well as illumination differences caused by topography. An average spectrum for the entire scene is then calculated from the normalized spectra. Finally, each normalized image spectrum is divided by the average spectrum. The resulting spectral values represent reflectance relative to the average spectrum, and in ideal cases should be comparable to true reflectance spectra. (Fig. 3)

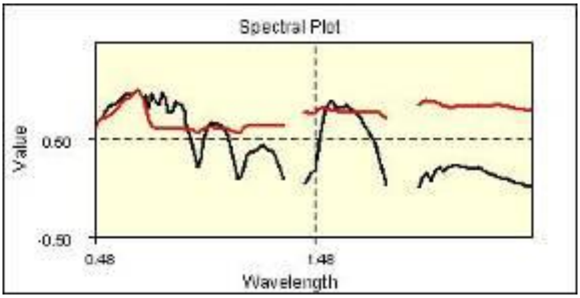

Fig 3 Raw radiance spectrum (black line) vs. calibrated to reflectance (red line) spectrum.

3.2 Data Dimensionality Reduction

Theoretically, using images with more bands should increase automatic classification accuracy. However, this is not always the case. Adjacent hyperspectral image bands are visually and numerically similar, and therefore contain much redundant information. Dimensionality reduction can be achieved in two different ways (Young, 1986). The first approach is to select a small subset of features which could contribute to class separability or classification criteria. This dimensionality reduction process is referred to as feature selection or band selection (Petridis, 2003, Charou, 2004). The other approach is to use all the data from original feature space and map the effective features and useful information to a lower-dimensional subspace. This method is referred to as feature extraction. The Principal Components (PCA) and the Minimum Noise Fraction (MNF) transforms are the standard methods for feature extraction. in hyperspectral imagery. The MNF is based on the Maximum Noise Fraction transformation described by (Green et al., 1988) Maximum Noise Fraction calculates an orthogonal set of components from a multivariate image, to maximise signal to noise ratio, instead of maximising variance as in the case of principal components analysis. The output MNF data is a series of uncorrelated bands in terms of increasing signal-to-noise (i.e. the first component contains the maximum noise). A variant of this method is employed in ENVI and TNTmips software but is called Minimum Noise Fraction and is given the same acronym MNF. Using the MNF a set of 10 components was produced. Various colour combinations using the MNF components were visually assessed. The (3= R, 2=G, 4=B, 1=I) combination gave satisfying results in identify marble formations (Fig 4). The boundaries of these formations are not well defined. This problem is solved when this picture is assessed together with the Matched Filtering result (Fig 5b).

3.3 Creation of a library with spectra of recognizable rock types.

Fig. 4 RGBI display of the first 4 MNF components (3= R, 2=G, 4=B, 1=I). Arrows show marble formations

An image derived spectral library was created using image spectra from relatively pure occurrences of 4 of the common rocks in the Naxos scene: granodiorite, migmatite, marble and basic rocks. Using various algorithms the similarity of each pixel spectrum of the research area and the selected rock type spectrum is calculated and a value is assigned to the pixel. A new image is created and the discrimination of the rock types is examined visually. Several mapping techniques were evaluated. The Spectral Angle Mapper (SAM) (Kruse et all 1993) algorithm treats target spectra and image spectra as vectors in n-dimensional spectral space. Each spectrum defines a point in spectral space, and this point can also be treated as the end of a vector that begins at the origin of the coordinate system. The angle between a pair of vectors is a measure of the similarity of the spectra; smaller spectral angles (dark tones) indicate greater similarity. This method is insensitive to differences in average brightness between spectra that may be due to topographic or sensor gain effects, because these factors change the length of the spectral vector, but not its orientation. The algorithm gave satisfactory results in discriminating granites, migmatites and basic/ultrabasic rocks while failed in discriminating marbles. The granodiorite boundaries can be depicted with relative success on the HYMAP image but they are diffused where they are covered by soil. Both amhibolite and diabase horizons appear with dark tones and this may due to the fact that there are common minerals between them and the granite, such as biotite, hornblende etc. The migmatites have common minerals with amphibolites and granites so dark tones appear over the last two rock types. Migmatite is relatively well defined in the NE part of the image where marble horizons are intercalated within the migmatites then the boundaries are diffused. The basic rocks are shown with dark tones in (Fig. 5a). These rock types are usually covered by soil as they are easily eroded. This makes their distinction not easy, so apart from two areas at the west and northern border of the map, other areas corresponding to Neogene sediments / melange and soils are also picked up.

For the discrimination of marbles the Matched Filtering Algorithm (MF) (Farrand and Harsanyi, 1994; Harsanyi and Chang, 1994), gave better results than SAM. The MF algorithm uses a Constrained Energy Minimization technique to assess the spectral composition of each image cell. Each image spectrum is assumed to be a linear mixture of a target spectrum and multiple unknown spectral signatures. The process identifies what proportion of each composite image spectrum could be produced by the target spectrum (end member). Brightest areas indicate a confided identification of the target material. The algorithm shows satisfactory degree of success for identifying marble zones which extend over micaschists, amphibolite and migmatite zones (Fig 5b). The individual marble horizons are shown only on certain places. Most probably this is related to the purity of minerals like calcite / dolomite which are the main constituents of the Naxos marbles as well as the soil and vegetation coverage. However, marble and not marble areas are sometimes confused on the rsulted by this algorithm image. This problem is solved when this picture is assessed together with the MNF color composite (Fig. 4). On the image in (Fig. 5b), marbles are shown with white tones.

Fig. 5a. Basic rocks (dark tones)

Fig. 5b. Marbles (bright tones)

3.4 Acquisition of characteristic minerals spectra from the USGS library.

Reflectance spectra of the materials in the USGS Spectral Library were used to locate and classify image cells with similar spectra. We used the SAM classification method as in the previous section but we selected USGS's library reflectance spectra instead of archived image spectra as end members. A series of material maps were produced showing the distribution of image cells matching the target spectrum. The similarity of each pixel spectrum is compared to the selected mineral spectrum of USSGS and a value is assigned to the pixel. A new image is created and the discrimination of the mineral is examined visually. Four minerals namely Muscovite, Amphibole, Biotite and Hornblende gave satisfactory results. Muscovite (Fig 6a) gave dark tones (high similarity) which dye slightly the zone of micaschists between the granite (NW of the image) and the amphibolites zone (center, SE). However, it verifies the presence of the lower grade zone, though its boundaries are diffused to both sides. Amphibole (Fig 6b) appears in the amphibolite and migmatite zones as well as in the granite showing similar «behavior» to hornblende. However it has better resolution of boundaries in soil covered areas and micashcist zone though with slightly less dark shades in amphibolite zone. Migmatite is not discernible relatively to amphibolite. Biotite shows a very similar image to that of hornblende and amphibole. Its distribution is within both granite and amphibolite zone and outside the lower grade mica (sericite) schist zone. Hornblende is projected on the granite, on the amphibolitic zone and the migmatites. The later is not clearly differentiated from amphibolites but the former are relatively darker. The lower grade metamorphic rocks, where muscovite is evidenced, are not dark shaded. Strike is well defined due to linear extent of amphibolitic intercalations

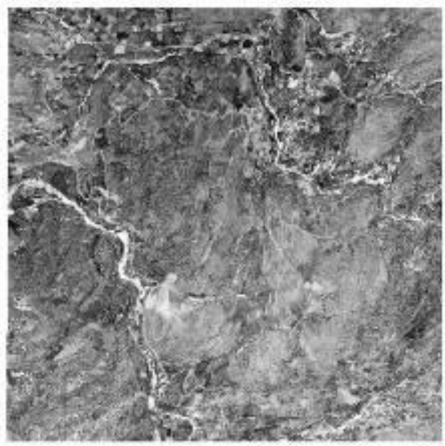

Fig6a Muscovite, dark tones

Fig6b. Amphibole: dark tones.

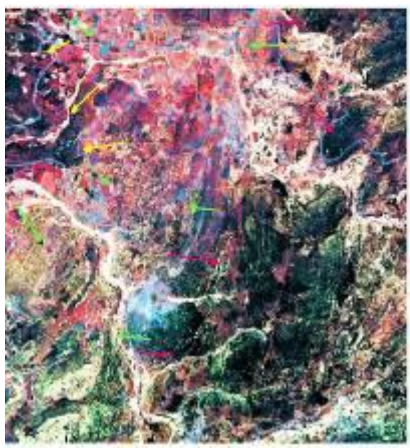

Figure 7a. Color Composite (R=Biotite, G=Quartz, B=Muscobite, I=Hornblende) Yellow arrows show the extend of the clean surface granodiorite. Red colors show apart from the low grade metamorphic zone, the soil covered ground. Dark colors show amphibolites. Green arrows show the low grade metamorphic rocks, while the purple arrow show the amphibolites.

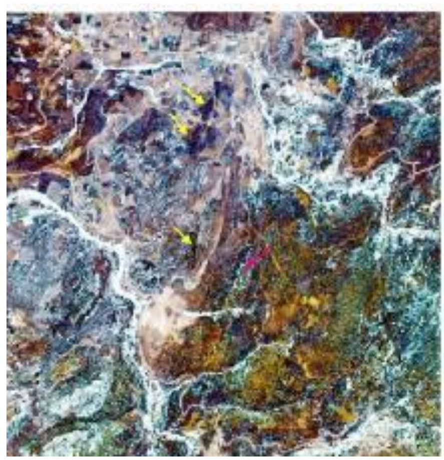

Fig 7b. This color combination (RGB. Epidote, Amphibole, Chlorite) shows the Basic rock occurrences. (yellow arrows) Purple arrows shows an amphibolitic horizon.

4. Conclusions

Early results of the HYMAP image analysis of Naxos scene show that the combined high spatial and spectral resolution of the data could be used to produce images of the composition and abundance of surface minerals thus making improvements of geological interpretation. Processing techniques that have been applied include integrated image processing / GIS vector data techniques. Combination of different resolution data using data fusion techniques proved to be effective as far as the interpretation of geologic features are concerned because complementary information for the same target is combined. The image derived mineral abundance maps could be integrated with other data sets and they could compliment field mapping by conventional techniques. Nevertheless, the human involvement in hyperspectral image analysis is still very high. The important decisions are still being made by a human operator concerning initial data quality assessment, data processing strategy, algorithms to apply, and features to extract.

Acknowledgement

The authors would like to thank the DLR for making the hyperspectral HYMAP image data available

References

Καραθανάση Β., Ρόκος Δ., Αργιαλάς Δ., Αναστασιάδης Μ., Τσακίρη Μ., Κουμαντάκης Ι., Κατέβας Ν., Καραγεώργης Α., 2005, «Υπερφασματικοί δέκτες και νερό: πρόγραμμα ΙΡΙΣ»,HELECO '05, Αθήνα 3-5 Φεβρ. 2005

Bachmann T. Donato, G. Lamela IEEE Trans. Geosci. & Rem. Sens.Vol. 40 No 10 pp 2313-2330

Bonneau M, Geyssant J, Lepvrier C (1978) Tectonique Alpine dans le massif d'Attique-Cyclades (Grece): plis couches kilometriques dans l'ile de Naxos. Consequences. Rev Geogr Phys Geol Dyn 20:109-122

Charou E., S. Petridis, M. Stefouli , O. D. Mavrantza, S. J. Perantonis Innovative feature selection used in multispectral imagery classification for water quality monitoring In XXth ISPRS Congress, Istanbul Turkey, pp. 1354-1358 July 2004 .

Echtler, H., Segl, K., Dickerhof, C., Chabrillat, S., and Kaufmann, H. (2002), Mineral identification and isograde mapping on the island of Naxos (Greece) using DAIS 7915 hyperspectral data. Proceedings of SPIE Remote Sensing for Environm. Monitoring, Geece, 23-27 September 2002, Vol. 4886, M. Ehlers (Ed.), SPIE, Bellingham, WA, pp.115-122.

Farrand, W.H., and J.C. Harsanyi, 1994, "Mapping Distributed Geological and Botanical Targets through Contstrained Energy Minimization," in Proc. Tenth Thematic Conference on Geologic Remote Sensing, San Antonio, TX, 9-12 May 1994, pp. I-419 - I-429.

Ganas, A., and Ferrier, G., 2002, Mapping of Diagnostic Clay Minerals in Epithermal Gold Deposits of Milos Island (Greece) using Hyperspectral Data from the DAIS Airborne Radiometer, Mineral Wealth, 122, 37 - 46.

Harsanyi, J.C., and C.I. Chang, 1994, "Hyperspectral Image Classification and Dimensionality Reduction: an Orthogonal Subspace Projection Approach," IEEE Trans. Geosci. & Rem. Sens., vol. 32, pp. 779-785.

Jansen J.B.H. 1973. Geological Map of Greece: Naxos Island, scale 1/50000. IGME, Athens.

Kruse, F.A., A.B. Lefkoff, J.W. Boardman, K.B. Heidebrecht, A.T. Shapiro, P.J. Barloon, and A.F.H. Goetz, 1993,"The Spectral Image Processing System (SIPS) – Interactive Visualization and Analysis of Imaging Spectrometer Data," Rem. Sens. Envir., vol. 44, pp. 145-163.

Lewis, M., 2001. Discriminating vegetation with hyperspectral imagery – what is possible? IEEE 2001 TGARSS, University of NSW, Sydney, Australia.

Petridis S., E Charou and S J. Perantonis "Non redundant feature selection of multiband remotely sensed images for land cover classification" In Tyrrhenian International Workshop on remote sensing Elba, Italy pp. 657-666, September 2003.

Green A. A., Berman, M., Switzer, P. and Graig, M.D. - A transformation for ordering multispectral data in terms of image quality with implications for noise removal. IEEE Trans. Geosci. & Rem. Sens (1988), pp 65-74.

Taylor G. R. and D. Vucovic "Mine Site Mapping with Hyperspectral Imagery" IEEE Trans. Geosci. & Rem. Sens 2001

Van der Meer, 5th EARSeL SIG IS workshop, April 2007, Bruges, Belgium http://5thearselsigis.vgt.vito.be/documents/Workshop_conclusions_5thearselsigis.pdf

Young, T.Y. and K.S. Fu. Handbook of Pattern Recognitions and Image Processing. College of Engineering, University of Miami,. Coral Gables, Florida, 1986.

Wijbrans JR (1985) Geochronology of metamorphic terrains by the Ar 4~ age spectrum method. PhD Thesis, Australian National University.